

# CURIOUS CONVERGENCE WITH HYPO-STATIC HYBRID EQUILIBRIUM MODELS

A.C.A. Ramsay<sup>1</sup>, J.P.B. Moitinho de Almeida<sup>2</sup> & E.A.W. Maunder<sup>3</sup>

1. Department of Civil & Structural Engineering, Nottingham Trent University, Burton St., Nottingham NG1 4BU, England.

2. Departamento de Engenharia Civil, Instituto Superior Técnico, Universidade Técnica de Lisboa, Av. Rovisco Pais, 1096 Lisboa Codex Portugal.

3. School of Engineering, University of Exeter, North Park Road, Exeter, EX4 4QF, England.

## SUMMARY

The paper describes an unexpected type of convergence behaviour occurring for a single, variable degree, primitive-type equilibrium element. For this element the number of independent stress fields is *less* than the number of independent boundary displacement variables that do not correspond to rigid element modes of displacement. This leads to the conclusion that the element is hypo-static and that, in the absence of self-stressing modes, no convergence can occur. Such 'conventional' counting procedures, do not, however, reveal the whole picture, and numerical determination of the rank of the coefficient matrix of the equilibrium equations shows that, in practice, self-stressing modes can and do exist in a model which would conventionally be described as hypo-static. The rank deficiency in the coefficient matrix is shown to be due to the fact that upon transformation, independent stress fields do not necessarily lead to independent boundary tractions. Generalisation to conventionally iso- and hyper-static models demonstrates that whenever the coefficient matrix is rank-deficient, spurious kinematic modes *co-exist* with self-stressing modes. The problem which reveals the curious convergence characteristics for the primitive-type element is re-solved using a macro-type element and it is seen that with the larger degree of hyper-staticity available to this element, strictly monotonic convergence characteristics are observed.

**KEY WORDS** hybrid-equilibrium finite elements, statically admissible, spurious kinematic modes, self-stressing modes

## INTRODUCTION

When faced with an unfamiliar type of finite element, confidence in its performance can be gained by testing it on a problem for which either the exact solution is known, or reliable results from another type of numerical approach are available. It was with this idea in mind that the variable degree quadrilateral primitive-type element described in reference [1] was tested. The problem examined is shown in Fig. 1.

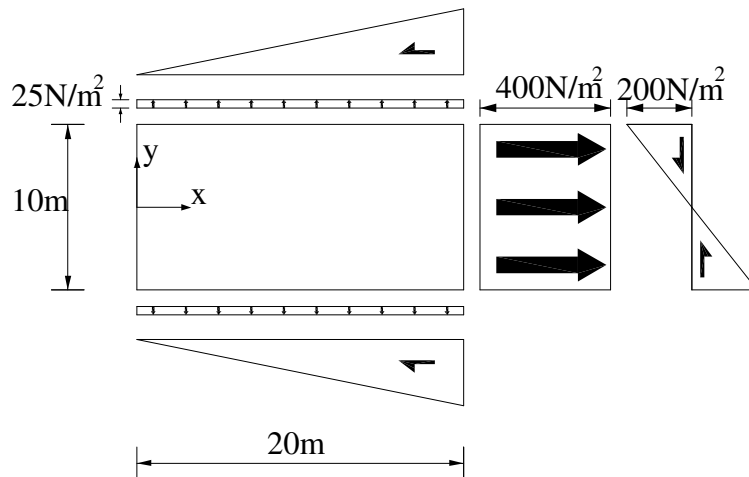


**Fig. 1. A plane problem**

The static boundary conditions are determined so as to be in equilibrium with the following stress field :

$$\begin{aligned}\sigma_x &= x^2 \\ \sigma_y &= y^2 \\ \tau_{xy} &= -2xy\end{aligned}\tag{1}$$

This stress field, whilst being statically admissible, is not kinematically admissible and is, therefore, invalid as the solution to the problem.

A plane stress constitutive relationship is used with a Young's modulus  $E = 210\text{N/m}^2$ , a Poisson's ratio  $\nu = 0.3$ , and a material thickness  $t = 0.1\text{m}$ . The problem was analysed using a single quadrilateral primitive-type equilibrium element of the type discussed in [1] and for varying degrees of approximation in the range  $2 \leq p \leq 10$  the finite element strain energies are given in Table 1. For a constant degree of approximation ( $p = 0$ ) the linear static boundary conditions (tangential component of the tractions - see Fig. 1) could not be equilibrated and for  $p = 1$  the applied tractions excited spurious kinematic modes. For these reasons results for the constant and linear cases are not available.

**Table 1. Strain energy for quadrilateral primitive-type element ( $Nm$ )**

| $p$   | 2         | 3         | 4         | 5         | 6         | 7         | 8         | 9         | 10        |
|-------|-----------|-----------|-----------|-----------|-----------|-----------|-----------|-----------|-----------|
| $U_h$ | 2048.2804 | 2048.2804 | 2048.2804 | 2048.2804 | 2042.1350 | 2042.1350 | 2041.6208 | 2041.6208 | 2041.6028 |

Note: The strain energy for the stress field of equation (1) is  $387125 / 189 \approx 2048.2804 Nm$ .

The results shown in Table 1 are plotted in Fig 2 where the 'exact' solution has been taken from a highly refined (equilibrium) finite element model reported in [2].

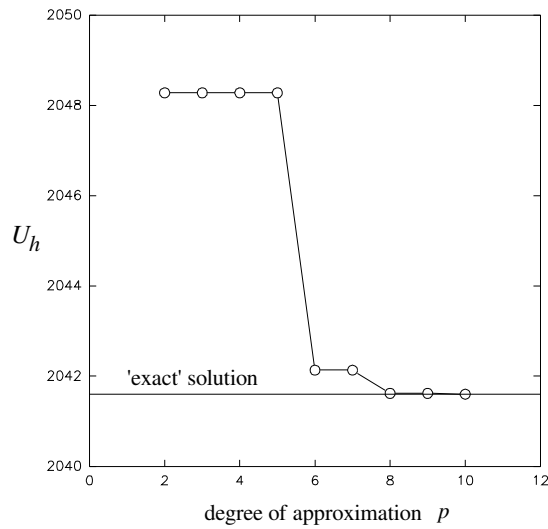


**Fig. 2. Convergence of strain energy for a primitive-type element**

The convergence of the strain energy with increasing degree of approximation is at first sight unexpected. Rather than the strictly monotonic convergence one might have predicted i.e.  $U_h|_{p=i+1} < U_h|_{p=i}$ , a step-wise convergence occurs for which the strain energy remains constant for certain ranges of the degree of approximation i.e.  $U_h|_{p=i+1} \leq U_h|_{p=i}$ . In order to provide an explanation for this behaviour it is necessary to summarise and examine the theory behind equilibrium elements.

### HYBRID EQUILIBRIUM ELEMENTS

A recent paper [3], in which the theoretical and practical aspects of this type of element are discussed, is used as the basis for the following summary. For a single primitive-type<sup>1</sup> equilibrium element,  $e$ , the equations of internal compatibility and boundary equilibrium are :

$$\begin{bmatrix} -\mathbf{F}^e & \mathbf{D}^{eT} \\ \mathbf{D}^e & \mathbf{0} \end{bmatrix} \begin{Bmatrix} \mathbf{s}^e \\ \mathbf{v}^e \end{Bmatrix} = \begin{Bmatrix} \mathbf{0} \\ \mathbf{g}^e \end{Bmatrix} \quad \begin{array}{l} \text{Compatibility} \\ \text{Equilibrium} \end{array} \quad \begin{array}{l} (2a) \\ (2b) \end{array}$$

where the various symbols have the following meanings :

$$\mathbf{F}^e = \int_{n_s \times n_s} \mathbf{S}^T \mathbf{f} \mathbf{S} de \quad \text{natural flexibility matrix} \quad (3a)$$

$$\mathbf{D}^e = \int_{n_v \times n_s} \mathbf{V}^T \mathbf{T} \mathbf{S} ds \quad \begin{array}{l} \text{coefficient matrix of the equations} \\ \text{of edge equilibrium} \end{array} \quad (3b)$$

$$\mathbf{g}^e = \int_{\partial e} \mathbf{V}^T \mathbf{t} ds \quad \text{applied edge tractions} \quad (3c)$$

and where :

$\mathbf{s}^e$  are the undetermined amplitudes of the  $n_s$  independent modes of stress which are statically admissible with zero body forces and are represented by the columns of the matrix  $\mathbf{S}$  ( $\boldsymbol{\sigma} = \mathbf{S}\mathbf{s}^e$ ), and

$\mathbf{v}^e$  are the undetermined amplitudes of the  $n_v$  independent modes of edge displacement which are represented by the columns of the matrix  $\mathbf{V}$  which include  $n_r$  rigid element modes of displacement.

The matrix  $\mathbf{f}$  is the material matrix relating strains ( $\boldsymbol{\epsilon}$ ) to stresses ( $\boldsymbol{\sigma}$ ) such that  $\boldsymbol{\sigma} = \mathbf{f}\boldsymbol{\epsilon}$  and the matrix  $\mathbf{T}$  relates stresses to boundary tractions ( $\mathbf{t}$ ) i.e.  $\mathbf{t} = \mathbf{T}\boldsymbol{\sigma}$ . The integrations  $de$  and  $ds$  are taken, respectively, over the volume, and around the boundary of the element.

Equilibrium between the applied edge tractions  $\mathbf{g}^e$  and the internal stress fields  $\boldsymbol{\sigma} = \mathbf{S}\mathbf{s}^e$  is expressed by equation (2b).

Dual to these are the following equations :

$$\mathbf{D}^{eT} \mathbf{v}^e = \boldsymbol{\delta}^e \quad (4)$$

which express compatibility between the element edge displacements  $\mathbf{v}^e$  and the element deformations  $\boldsymbol{\delta}^e$ .

The  $n_r$  rigid element modes of edge displacement satisfy the homogeneous form of equation (4). In addition, for the hypo-static case where  $n_v - n_r > n_s$  there are further modes of displacement satisfying the homogeneous form of (4). These modes of displacement are called *spurious kinematic modes* and the number of these is given as :

$$n_{skm} \geq n_v - n_r - n_s \quad (5)$$

For each spurious kinematic mode there is a corresponding mode of edge traction which is inadmissible. Inequality (5) becomes an equality when the  $n_s$  columns of the matrix  $\mathbf{D}^e$  are independent. It is easy to fall into the trap of assuming that, since the stress fields (the columns of  $\mathbf{S}$ ) are *defined* as being independent, then the tractions corresponding to these stress fields (the columns of  $\mathbf{TS}$ ) are also independent. This, however, is not the case as will be demonstrated. If the matrix  $\bar{\mathbf{D}}^e$  is defined as in (3b) except with  $\mathbf{V}$  replaced by  $\bar{\mathbf{V}}$ , which excludes rigid element modes, then the rank deficiency of  $\bar{\mathbf{D}}^e$  is defined as  $s$ , and (5) may be written as :

$$n_{skm} = n_v - n_r - n_s + s \quad (6)$$

In addition to affecting the number of spurious kinematic modes,  $s$  also affects the number of *self-stressing modes* i.e. the number of modes of stress that satisfy the homogeneous form of the equilibrium equations (2b). For the hypo-static case being considered the number of self stressing modes will be given by :

$$n_{ssm} = s \quad (7)$$

This leads to the, perhaps surprising, conclusion that an element which is conventionally described as hypo-static can possess self-stressing modes. These self-stressing modes result from the rank deficiency of  $\bar{\mathbf{D}}^e$  and explain why the oft quoted *stability criterion*, which states that the number of independent stress fields should satisfy  $n_s \geq n_v - n_r$ , see [4] (p388) for example, is a necessary but not sufficient condition to guarantee a formulation free from spurious kinematic modes.

It is possible to generalise this idea to models which are conventionally described as hyper- and iso-static. This has been done in Table 2, which defines the descriptors hyper-, iso-, and hypo-static in terms of the independent characteristic numbers, and is illustrated schematically in Fig. 3.

**Table 2. The effect of rank deficiency ( $s$ ) on the dependent characteristic numbers**

| Conventional description | Independent characteristic numbers<br>(relationship between) | Dependent characteristic numbers |                       |
|--------------------------|--|----------------------------------|-----------------------|
|                          |  | $n_{ssm}$                        | $n_{skm}$             |
| hyper-static             | $n_s > n_v - n_r$  | $n_s - n_v + n_r + s$            | $s$                   |
| iso-static               | $n_s = n_v - n_r$  | $s$                              | $s$                   |
| hypo-static              | $n_s < n_v - n_r$  | $s$                              | $n_v - n_r - n_s + s$ |

<sup>1</sup>the description *primitive-type* distinguishes these elements from *macro-type* elements which are assemblies of the basic or primitive-type element.

In Table 2 the dependent characteristic numbers ( $n_{ssm}$  and  $n_{skm}$ ) are defined in terms of the independent characteristic numbers and the rank deficiency  $s$  for the three conventional descriptions of an element. It is seen that both the number of spurious kinematic modes and the number of self-stressing modes are increased by the value of  $s$  and that models in which spurious kinematic modes and self-stressing modes co-exist are perfectly feasible. Fig. 3 shows the *normal form*, [5], of the coefficient matrices for the equilibrium and compatibility equations for the three conventional model descriptions after extraction of the  $n_r$  rigid element modes of edge displacement from  $\mathbf{V}$ . The independent columns of the matrices in Fig. 3 are indicated 'IND' and have unity on the leading diagonal with zeros elsewhere.

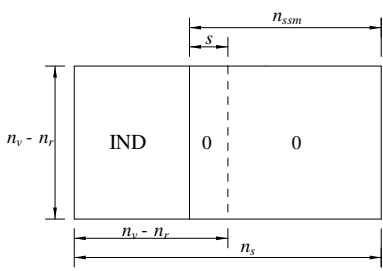
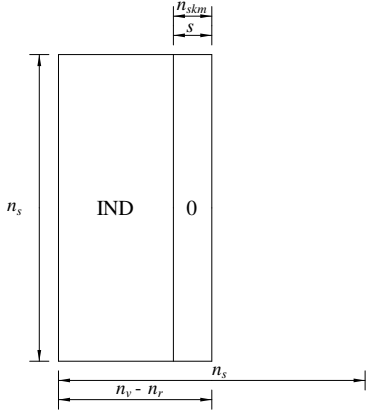
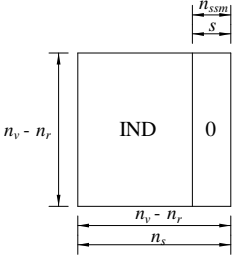
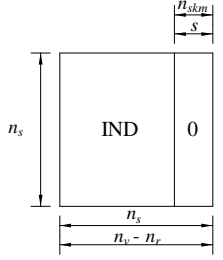
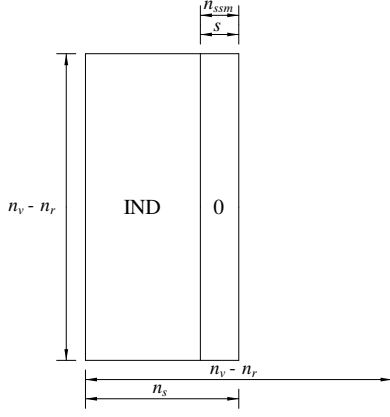
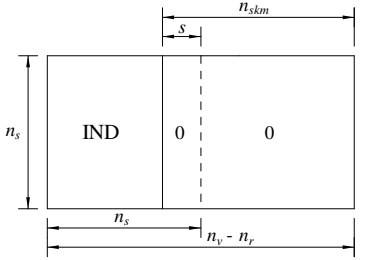
| Conventional description | Normal form of Equilibrium matrix ( $\bar{\mathbf{D}}^e$ )                          | Normal form of Compatibility matrix ( $\bar{\mathbf{D}}^{eT}$ )                       |
|--------------------------|---|---|
| hyper-static             |    |    |
| iso-static               |  |  |
| hypo-static              |  |   |

Fig. 3. A schematic diagram of the normal form of the coefficient matrices  $\bar{\mathbf{D}}^e$  and  $\bar{\mathbf{D}}^{eT}$

The aforementioned considerations apply equally well to a number of different types of element. Let us now consider the situation that occurs for plane equilibrium elements with stress fields and boundary displacements in polynomial form. To ensure equilibrium at the element boundary the degree of the polynomial stress field defined within the element must be equal to the degree of polynomial displacement defined on the boundaries of the element. The term *degree of approximation*  $p$  is thus used unambiguously to describe both the degree of polynomial stress field assumed within the element and the degree of polynomial displacement assumed on the boundary. For a plane problem ( $n_r = 3$ ) with polynomial approximations, the independent characteristic numbers for the quadrilateral primitive-type element are written in terms of  $p$  as :

$$n_v = 4 \times 2(p+1) \tag{8a}$$

$$n_s = \frac{1}{2}(p+1)(p+6) \tag{8b}$$

At present, the *a priori* prediction of the magnitude of  $s$  is not generally possible and, therefore, may only be determined numerically after formation of the  $\bar{\mathbf{D}}^e$  matrix. For the single quadrilateral primitive-type element the magnitudes of the various characteristic numbers have been observed in numerical trials, and are given in Table 3.

**Table 3. Quadrilateral primitive-type element characteristics ( $n_r = 3$ )**

| $p$ | $n_v$ | $n_s$ | $s$ | $n_{skm}$ | $n_{ssm}$ | -/+ | class <sup>2</sup> |
|-----|-------|-------|-----|-----------|-----------|-----|--------------------|
| 0   | 8     | 3     | 0   | 2         | 0         | -   | II                 |
| 1   | 16    | 7     | 0   | 6         | 0         | -   | II                 |
| 2   | 24    | 12    | 0   | 9         | 0         | -   | II                 |
| 3   | 32    | 18    | 0   | 11        | 0         | -   | II                 |
| 4   | 40    | 25    | 0   | 12        | 0         | -   | II                 |
| 5   | 48    | 33    | 0   | 12        | 0         | -   | II                 |
| 6   | 56    | 42    | 1   | 12        | 1         | -   | IV                 |
| 7   | 64    | 52    | 3   | 12        | 3         | -   | IV                 |
| 8   | 72    | 63    | 6   | 12        | 6         | -   | IV                 |
| 9   | 80    | 75    | 10  | 12        | 10        | -   | IV                 |
| 10  | 88    | 88    | 15  | 12        | 15        | +   | IV                 |

The penultimate column of this table indicates whether the model (a single element in this instance) is hypo-static (-) or hyper-static (+); in this case there are no examples of an iso-static model. The shaded portion of the table highlights the range of degree of approximation for which  $s$  is non-zero and where spurious kinematic modes co-exist with self-stressing modes. It should be noted that despite the existence of spurious kinematic modes, solutions are possible within the range of degree of approximation  $2 \leq p \leq 10$ . This demonstrates the point that whilst spurious kinematic modes certainly do lead to the existence of inadmissible modes of applied traction and a rank-deficient stiffness matrix (see [3])

<sup>2</sup> This column (and the columns of Table 4 headed 'class') indicates the class of structural assembly following the classification of Pellegrino [6].

for the definition of the stiffness matrix), provided the applied tractions are admissible ('consistent' in matrix terminology) a solution is achievable if an appropriate (singular) equation solver is used [1,2]. This solution, whilst being non-unique in terms of edge displacements, will be unique in terms of element stresses. For the problem investigated in this paper (see Fig. 1) the static boundary conditions lead to applied tractions which are admissible for  $p \geq 2$ .

### DISCUSSION & CONCLUSIONS

It is now possible to give an explanation for the curious convergence characteristics described in the introduction. Firstly it is seen that for the range of degree of approximation  $2 \leq p \leq 5$  the finite element strain energy (as given in Table 1) is independent of  $p$ . In this range it is observed that the strain energy is equal to that of the stress field given in equation (1). The reason for this last point is due to the fact that the element is giving an equilibrium solution and one which satisfies the boundary conditions exactly. The explanation why the solution remains independent of  $p$  for the given range becomes evident on closer inspection of Table 3. It is seen that in the given range of degree of approximation there are no self-stressing modes. Since the finite element solution already satisfies the static boundary conditions for  $p = 2$ , there can be no decrease<sup>3</sup> in the finite element strain energy until a self-stressing mode is made available. Thus, for  $p = 6$  the sudden decrease in strain energy is due to the availability of a (single) self-stressing mode.

As the degree of approximation is increased from  $p = 6$  to  $p = 7$ , no change in the value of the strain energy is observed despite the three additional self-stressing modes made available to the model. This is reasonable since the existence of self-stressing modes, whilst being necessary, is not a sufficient condition for the reduction of strain energy i.e. whilst these modes may be available, they may not actually be used.

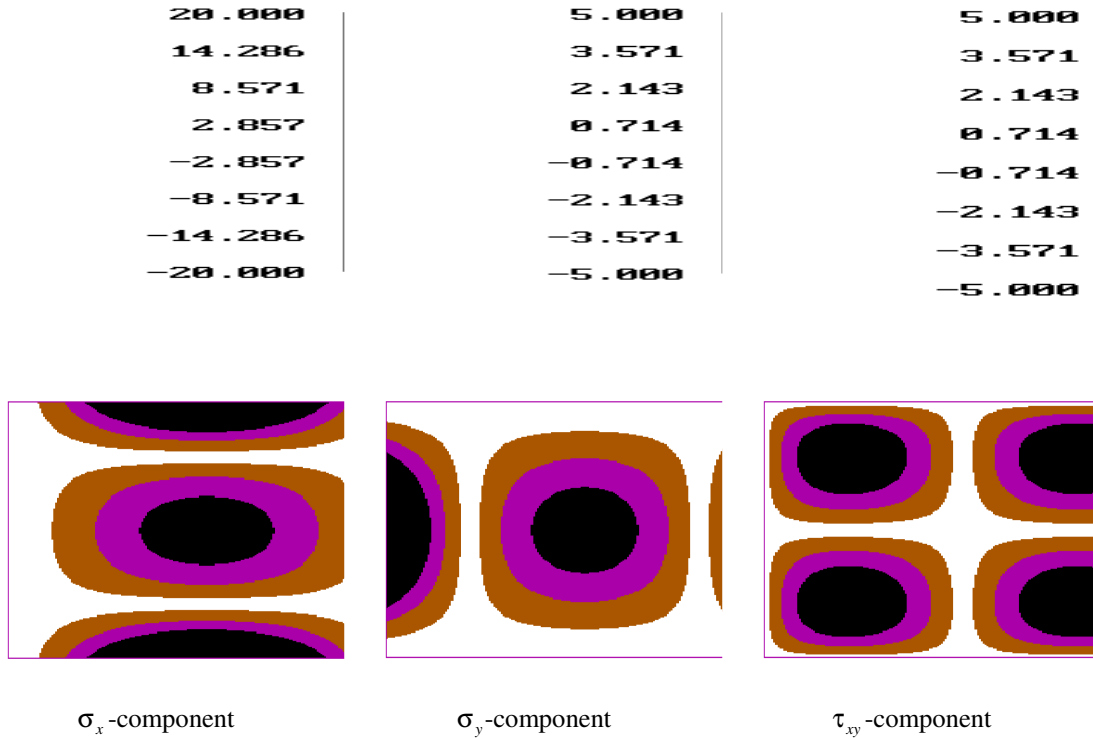
A similar rationale holds for the higher values of  $p$ . As the degree of approximation is increased from  $p = 7$  to  $p = 8$  some of the three additional self-stressing modes are utilised to improve the solution. For degree of approximation in the range  $8 \leq p \leq 9$  no change is detected and finally, for  $p = 10$  a further (small) decrease in strain energy is observed giving a solution which is within 0.00003% of the exact solution [2]. It is observed that convergence only occurs with even degrees of approximation. This can be explained by noting that anti-symmetric self-stressing modes are inadmissible in a problem, such as this one, which exhibits symmetry.

$$\sigma_x|_{x=0} = 0, \sigma_x|_{x=20} = 0, \sigma_y|_{y=\pm 5} = 0, \tau_{xy}|_{x=0} = 0, \tau_{xy}|_{x=20} = 0, \tau_{xy}|_{y=\pm 5} = 0 \quad (9)$$

As an example of a self-stressing mode the one occurring when  $p = 6$  is shown in Fig. 4. This figure is a plot of the stress field given in equation (1) subtracted from the finite element stress field for  $p = 6$ . A self-stressing mode has zero corresponding boundary tractions and this can be observed through the stresses on the boundaries which satisfy the conditions given in (9).

---

<sup>3</sup>For force driven problems such as the one considered here, equilibrium models yield a value of strain energy which is an upper bound to the exact value.



Note: the maximum magnitudes of the stresses for the 'exact' solution are in the order of 400, 25, and 200 respectively for the three components of stress  $\sigma_x$ ,  $\sigma_y$ , and  $\tau_{xy}$ .

**Fig. 4. A self-stressing mode**

The curious convergence characteristics discussed in this paper occurred for the particularly extreme case of a single element model. Whilst it might not seem unreasonable to have tackled this problem with a single element (the material properties and boundary conditions are continuous and the geometry is simple), it is likely that had a mesh of such elements been used the curious convergence would not have occurred or, if it had, it would have been less extreme. The reason for this is that whereas for the single element self-stressing modes only become available at a relatively high degree of approximation ( $p = 6$  in this case), with meshes of elements self-stressing modes can be set up within groups or patches of elements and these will occur at lower degrees of approximation. Consider, for example the additional self-stressing modes that may occur in a patch of four elements as illustrated in Fig. 5 which shows examples of possible self-stressing interactions within a patch of four elements.

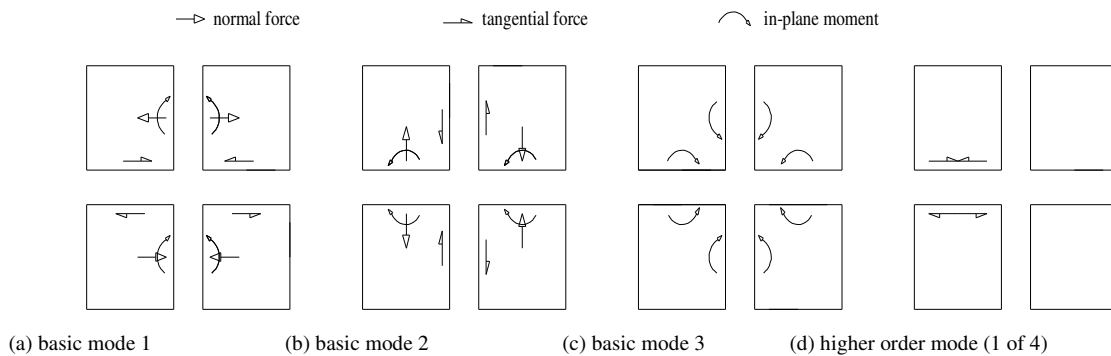


**Fig. 5. Illustration of self-stressing modes within a patch of four primitive-type elements**



The modes are categorised as *basic* (a, b & c) and *higher order* (d), [7]. The distinction being made here is that a higher order mode is self-equilibrating on a single interelement boundary. There are four such modes in the group of elements shown, corresponding to the four interelement boundaries.

In the present state of knowledge, primitive-type elements, whilst forming an interesting area of research, are of limited practical utility due to the existence of spurious kinematic modes which occur at the element level (see row 5 of Table 3) and which may propagate unpredictably to the model boundaries leading to cases where not all the possible modes of applied loading are admissible. Macro-elements, on the other hand, which are groups of primitive-type elements judiciously assembled so as to eliminate the effect of spurious kinematic modes on the boundaries of the assembly, are robust in the sense that for an arbitrary mesh of such elements all the possible modes of applied loading are admissible [2,3].

Whilst it would be incorrect to give the impression that the curious convergence characteristics reported in this paper are peculiar to the quadrilateral primitive-type element alone, it is fair to say, based on the aforementioned argument of increasing hyper-staticity with increasing *h*-type refinement, that this behaviour would be less likely to occur for the quadrilateral macro-type element. This point can be demonstrated by comparing the element characteristic numbers for the two elements. Table 4 lists the element characteristics for a quadrilateral macro-type element. The quadrilateral macro-type element is constructed from four triangular primitive-type elements and the construction is defined by the position of the assembly point *P* as shown in Fig. 6.

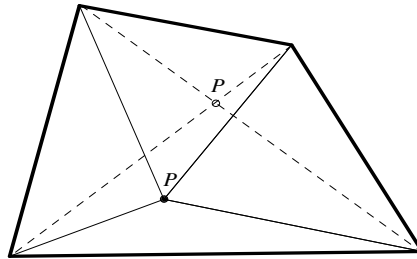


**Fig. 6. Quadrilateral macro-type element**

The characteristics of the macro-type element are dependent on whether the assembly point *P* is located at the intersection of the diagonals (as shown in dotted lines in Fig. 6) or is located away from this point [2,3]. For a plane problem ( $n_r = 3$ ) with polynomial approximation, the independent characteristic numbers for the quadrilateral macro-type element are :

$$n_v = 4 \times 2(p+1) \quad (10a)$$

$$n_s = \frac{4}{2}(p+1)(p+6) - 8(p+1) + (c) \quad (10b)$$

In equations (10), the macro-type element has been considered as a single element with piecewise statically admissible stress fields and the relationships given in Table 2 remain true. The term  $c$  in equation (10b) depends on the position of the assembly point. For  $P$  at the intersection of the diagonals  $c = 1$ , and for any other position  $c = 0$ .

**Table 4. Quadrilateral macro-type element characteristics ( $n_r = 3$ )**

|     |       | $P$ at intersection of diagonals ( $c = 1$ ) |     |           |           |       | $P$ not at intersection of diagonals ( $c = 0$ ) |     |           |           |       |
|-----|-------|--|-----|-----------|-----------|-------|--|-----|-----------|-----------|-------|
| $p$ | $n_v$ | $n_s$  | $s$ | $n_{skm}$ | $n_{ssm}$ | class | $n_s$  | $s$ | $n_{skm}$ | $n_{ssm}$ | class |
| 0   | 8     | 5  | 0   | 0         | 0         | I     | 4  | 0   | 1         | 0         | II    |
| 1   | 16    | 13   | 0   | 0         | 0         | I     | 12   | 0   | 1         | 0         | II    |
| 2   | 24    | 25   | 0   | 0         | 4         | III   | 24   | 0   | 0         | 3         | III   |
| 3   | 32    | 41   | 0   | 0         | 12        | III   | 40   | 0   | 0         | 11        | III   |
| 4   | 40    | 61   | 0   | 0         | 24        | III   | 60   | 0   | 0         | 23        | III   |
| 5   | 48    | 85   | 0   | 0         | 40        | III   | 84   | 0   | 0         | 39        | III   |
| 6   | 56    | 113  | 0   | 0         | 60        | III   | 112  | 0   | 0         | 59        | III   |
| 7   | 64    | 145  | 0   | 0         | 84        | III   | 144  | 0   | 0         | 83        | III   |
| 8   | 72    | 181  | 0   | 0         | 112       | III   | 180  | 0   | 0         | 111       | III   |
| 9   | 80    | 221  | 0   | 0         | 144       | III   | 220  | 0   | 0         | 143       | III   |
| 10  | 88    | 265  | 0   | 0         | 180       | III   | 264  | 0   | 0         | 179       | III   |

For the macro-type element considered as a whole, the matrix  $\bar{\mathbf{D}}^e$  possesses full rank, i.e.  $s = 0$ , independent of the degree of approximation and the position of the assembly point  $P$ . It is seen that whereas the quadrilateral primitive-type element remained effectively<sup>4</sup> iso-static up to a degree of approximation  $p = 6$  (see Table 3), the macro-type element is effectively hyper-static for any degree of approximation greater than one, and that for a given degree of approximation (greater than one) the number of self-stressing modes in the macro-type element, which is more elaborate, is significantly greater than for a single primitive-type element.

Of course, the existence of self-stressing modes does not guarantee their use in the solution as has already been demonstrated. In order to show that they are actually used, the problem discussed in the introduction will be re-solved using a single (variable degree) quadrilateral macro-type element. The finite element strain energies are recorded in Table 5 and have been plotted in Fig. 7 and show a strictly monotonic convergence of the type one might expect to see.

**Table 5. Strain energy for quadrilateral macro-type element ( $Nm$ )**

| $p$   | 2         | 3         | 4         | 5         | 6         | 7         | 8         | 9         | 10        |
|-------|-----------|-----------|-----------|-----------|-----------|-----------|-----------|-----------|-----------|
| $U_h$ | 2042.5410 | 2041.8020 | 2041.6340 | 2041.6116 | 2041.6041 | 2041.6027 | 2041.6024 | 2041.6023 | 2041.6023 |

Note: these results are for  $P$  positioned at the intersection of the diagonals.

<sup>4</sup>By *effectively* it is meant that the actual number of self-stressing modes is used rather than that predicted by a simple counting procedure.

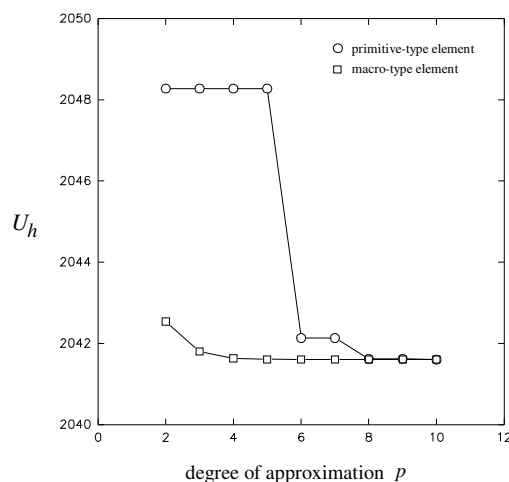


**Fig. 7. Convergence of strain energy for a macro-type element**

Note that whereas for  $p = 1$  a solution was not attainable with the primitive-type element due to the existence of spurious kinematic modes, provided the assembly point  $P$  is located at the intersection of the diagonals a solution for  $p = 1$  is possible with the macro-type element. For  $p = 1$  and with  $P$  at the intersection of the diagonals, the finite element strain energy is  $2168.6508Nm$ .

In conclusion, it has been illustrated how the conventional descriptors for describing equilibrium models need to be used with caution. Independently defined stress fields do not guarantee that corresponding boundary tractions are independent, and in the event that they are not, the coefficient matrix of the equilibrium equations becomes rank-deficient. This results in an increase in both the number of spurious kinematic modes *and* the number of self-stressing modes by the degree of the rank deficiency and leads to situations where such modes can co-exist. The rank deficiencies reported in this paper have been determined numerically and further work remains to be done before an *a priori* prediction of the rank of the coefficient matrix can be made.

**Acknowledgement** - The idea for this paper was conceived by the first author during a post-doctoral research year at the Departamento de Engenharia Civil, Instituto Superior Técnico, Universidade Técnica de Lisboa, Lisboa, Portugal and was funded through a European Grant under the auspices of the *Human, Capital & Mobility Network 'Advanced Finite Element Solution Techniques on Innovative Computer Architectures'* - PL930382. The first author would like to record his gratitude to the people and organisations that made this opportunity possible.

## REFERENCES

1. J.P.B. Moitinho de Almeida and J.A. Teixeira de Freitas, 'Alternative approach to the formulation of hybrid equilibrium finite elements', *Computers and Structures*, **40**(4), 1043-1047 (1991).
2. A.C.A. Ramsay, *Robust Variable Degree Equilibrium Elements: their formulation and application*, Post doctoral thesis, I.S.T. Technical University of Lisbon, Portugal, 1995.
3. E.A.W. Maunder, J.P.B. Moitinho de Almeida and A.C.A. Ramsay, 'A General Formulation of Equilibrium Macro-Elements with Control of Spurious Kinematic Modes: the exorcism of an old curse', *Int. J. Numer. Meth. Engng.*, **39**, 3175-3194 (1996).
4. O.C. Zienkiewicz and R.L. Taylor, *The Finite Element Method*, 4th Ed, McGraw-Hill, 1989.
5. S. Barnett, *Matrices: Methods & Applications*, Clarendon Press, 1990.
6. S. Pellegrino, 'Structural Computations with the Singular Value Decomposition of the Equilibrium Matrix', *Int. J. Solids Structures*, **30**(21), 3025-3035 (1993).
7. E.A.W. Maunder and G.J. Savage, 'A Graph-Theoretic Model for Finite Elements with Side Variables', *Civil Engineering Systems*, **2**, 111-141, (1994).